Energy Engineering

Tech Science Press

https://doi.org/10.32604/ee.2026.077390

ARTICLE

A Spatiotemporal Collaborative Framework for Dynamic Cluster Partitioning in EV/EC-Integrated Distribution Networks

Fukang Zhang, Yang Wang*, Runtian Tang and Zhixin Yun

School of Electrical and Information Engineering, Jiangsu University, Zhenjiang, China

*Corresponding Author: Yang Wang. Email: wangjust@ujs.edu.cn

Received: 08 December 2025; Accepted: 02 February 2026; Published: 27 April 2026

ABSTRACT: The large-scale integration of electric vehicle (EV) and exchange stations (EC) into distribution networks introduces strong spatiotemporal load fluctuations and charging capacity constraints, leading to frequent voltage violations and reduced control flexibility. Traditional centralized control approaches face critical limitations, including high communication latency and computational complexity. To address these challenges, this paper proposes a Hybrid Intelligence (HI)-driven framework for distribution networks, which explicitly considers EV/EC charging power limits, cluster-level resource balance, and voltage security constraints. By incorporating spatiotemporal characteristics with intelligent optimization techniques, a Variant Monte Carlo Sampling (VMCS) algorithm is developed to generate the initial node partitions. These partitions are further refined using a Capacity-Corrected K-means Extension combined with Simulated Annealing Optimization (CCE-SAO), resulting in an optimized cluster configuration. A two-layer control architecture, termed "spatiotemporal collaborative optimization—distributed iteration," is established to effectively address the drawbacks of traditional static clustering methods in large-scale systems, such as vulnerability to local optima and limited adaptability. This enhances global optimization under complex operational scenarios. Simulation results on the IEEE 33-bus and IEEE 123-bus test systems show that the proposed HI-based method effectively improves voltage quality. In the IEEE 33-bus system, the voltage deviation at the most fluctuating node is reduced by 30% compared with conventional K-means clustering and by 40% compared with centralized control under peak load conditions, validating the effectiveness of the proposed framework for future distribution networks with large-scale EVEC integration.

KEYWORDS: Cluster partitioning; hybrid intelligent; EV/EC; distribution networks

1 Introduction

As electric vehicle (EV) penetration rises, the large-scale integration of electric vehicle and exchange stations (EV/EC) into distribution networks poses significant technical challenges. The strong spatiotemporal randomness and clustering characteristics of EV/EC loads often cause frequent voltage fluctuations and violations. When penetration exceeds 15%, the voltage stability index may drop below the critical threshold [1,2]. Meanwhile, the idle battery capacity at exchange stations during off-peak hours provides significant dispatchable potential. As shown in [3], these batteries can connect to the grid, with part of their capacity used for peak shaving and valley filling [4], thereby improving reliability and resilience while unlocking flexible resources for future power systems. However, traditional centralized control struggles to accommodate dynamic EV/EC loads due to large-scale coordination, high computational costs, and long communication delays. Their reliance on static partitioning further limits adaptability to long-term

regulation tasks [5]. To address these issues, recent studies propose clustering EV/EC, Energy Storage System (ESS), and Static Var Compensator (SVC)—devices with complementary electrical properties—into autonomous control groups. Distributed optimization reduces control dimensionality while enhancing flexibility and scalability of the system [6].

Despite extensive studies on cluster partitioning in distribution networks, existing methods remain inadequate for scenarios with large-scale EV/EC integration, primarily due to insufficient consideration of charging demand uncertainty, capacity constraints, and long-term dynamic adaptability. From the perspective of clustering metrics, current approaches can be broadly categorized into topology-based, static resource-based, and dynamic temporal methods. Topology-based metrics, such as K-means, rely mainly on electrical distance or network structure, which enables simple implementation but neglects the strong spatiotemporal randomness and aggregation effects of EV/EC charging demand. As a result, clusters formed under such metrics often fail to maintain voltage stability during high-penetration charging periods. Static resource-based metrics, including power balance, node affiliation, and capacity indices proposed in [7–9], incorporate physical resource information and perform well under steady-state operating conditions. However, these methods typically model regulation capacity as a static snapshot and overlook the time-varying nature of EV/EC charging and discharging behaviors. As reported in [10], their adaptability degrades by up to 45% over a 24-h horizon, indicating limited effectiveness for long-term regulation in systems dominated by flexible and intermittent EV loads. Dynamic temporal metrics attempt to capture load or renewable fluctuations over time [11], but most existing studies focus on demand variation alone and rarely integrate EV charging power limits, exchange station capacity boundaries, or the coupling between charging and discharging processes, which are critical for realistic EV/EC-dominated networks. From the algorithmic perspective, conventional clustering methods such as K-means [12] and K-medoids [13] are computationally efficient but highly sensitive to initial conditions and prone to local optima, leading to poor convergence and scalability in large-scale networks. U-SPEC [14] improves computational efficiency for large systems but sacrifices clustering accuracy in medium- and small-scale networks, limiting its applicability under varying EV/EC penetration levels. Probabilistic approaches, such as Monte Carlo-based methods [15], enhance global exploration capability but generally ignore spatiotemporal coupling and capacity-constrained regulation requirements, resulting in clusters that are difficult to adapt to dynamic charging scenarios. Collectively, these limitations reveal a critical gap in existing studies: the lack of a clustering framework that jointly accounts for EV/EC charging demand uncertainty, capacity-constrained regulation resources, and spatiotemporal adaptability, which motivates the hybrid intelligence–based clustering and optimization approach proposed in this paper.

To overcome these limitations, this paper proposes a Hybrid Intelligent (HI) algorithm that integrates spatiotemporal features. Here, 'Intelligence' specifically refers to the evolutionary optimization capability introduced by the genetic mutation and simulated annealing mechanisms. A hierarchical, staged optimization framework with dual-layer control achieves dynamic adaptability and global convergence. In this framework, exchange stations act both as loads and storage units. First, a collaborative index system quantifies spatial balance and net compensation capacity of initial nodes, ensuring a strong and adaptable starting configuration. Building on the static power balance in [7], a time-coupling factor captures cluster dynamics, producing a time-coupled index that balances topological constraints with regulation capability. A Variant Monte Carlo Sampling (VMCS) algorithm generates optimal initial node distributions, enhanced with genetic mutation for search efficiency. Then, a Capacity-Corrected K-means Extension with Simulated Annealing Optimization (CCE-SAO) ensures rapid convergence to global optima, forming a two-layer scheme of "spatiotemporal collaborative optimization—distributed iteration." Using the IEEE 33-bus and 123-bus systems, we test the method under large-scale EV/EC integration and validate its feasibility through a

cluster autonomy evaluation. Future work will extend the model to include communication delays, enabling systematic analysis of their impact on scheduling efficiency and cluster partitioning.

The remainder of this paper is organized as follows: Section 2 establishes a multidimensional index system for both initial allocation and final cluster division. Section 3 presents the HI algorithm, integrating VMCS and CCE-SAO for cluster formation. Section 4 evaluates the method on IEEE 33-bus and 123-bus systems and compares it with static methods such as K-means, showing superior adaptability under dynamic conditions.

2 Cluster Partitioning Metrics

2.1 Cluster Initial Node Allocation and Partitioning Metrics

2.1.1 Initial Node Distribution Metrics

To ensure the clarity of the symbols used, a variable table has been provided in Appendix A Table A1.

The spatial distribution of initial nodes plays a critical role in determining the disturbance resilience of clusters. When multiple initial nodes are concentrated in a localized region of the network, it may result in blurred cluster boundaries and increased complexity in power interactions. To mitigate the risk of cluster overlap due to uneven node placement, the spatial dispersion of initial nodes is quantified based on topological distance. Accordingly, a topology-based distribution index is introduced to assess the uniformity of initial node allocation across the system. A higher index value indicates a more evenly distributed initial node configuration among clusters. The metrics is defined as follows:

$$d_{\min} = \min\left[\min_{j\neq i}\left(topo_{i,j}, \forall j\right)\right]_{i} \tag{1}$$

$$R_{\text{distance}} = 1 - e^{-d_{\min}} \tag{2}$$

where $topo_{i,j}$ denotes the topological distance between the initial nodes of cluster i and those of cluster j, the shortest path length in an undirected network graph measured by the number of edges.

2.1.2 Net Compensation Capability of Initial Nodes

The power regulation margin of initial nodes is essential for maintaining cluster autonomy. Insufficient compensation capacity may lead to localized power deficits and increased reliance on inter-cluster support during the expansion phase. To address this, nodes with higher compensation capabilities should be prioritized as core cluster members. A corresponding index is proposed to quantify the power support potential of candidate nodes, ensuring that each initial node possesses adequate capacity to meet the demands of subsequent node allocation. The metrics is defined as follows:

$$P_{\text{net}}(k) = \sum_{i\in I_k}\sum_{t\in T_{in}}\left[P_{\text{sup}}(i,t) - P_{\text{load}}(i,t)\right] \tag{3}$$

$$Q_{\text{net}}(k) = \sum_{i\in I_k}\sum_{t\in T_{in}}\left[Q_{\text{sup}}(i,t) - Q_{\text{load}}(i,t)\right] \tag{4}$$

$$R_{\text{net}} = \frac{\eta_1}{K}\sum_{k=1}^{K}\text{normalize}\left(P_{\text{net}}(k)\right) + \frac{\eta_2}{K}\sum_{k=1}^{K}\text{normalize}\left(Q_{\text{net}}(k)\right) \tag{5}$$

where $P_{\text{sup}}(i, t)$ (W) is the active power compensation capacity of node i at time t. $P_{\text{load}}(i, t)$ (W) is the active power load of node i at time t. I_k is the set of initial nodes in cluster k. T_{in} is the time interval for cluster partitioning, set to 24 h. $P_{\text{net}}(k)$ (W) and $Q_{\text{net}}(k)$ (W) are the total net active and reactive compensation

capacities of the initial nodes in cluster k over the period. normalize() is the normalization operator. η_1 and η_2 are weight coefficients; and K is the total number of clusters.

2.1.3 Comprehensive Metrics for Initial Cluster Node Allocation

Initial nodes must balance topological dispersion with sufficient power capacity. Maximizing spatial dispersion minimizes inter-cluster coupling and interference, while robust compensation capacity ensures seamless node assignment during cluster formation. However, a trade-off exists: nodes with wide spatial separation often exhibit limited compensation potential, whereas those with strong compensation capability tend to be geographically clustered. To reconcile these objectives, this study introduces a dynamic weighting coordination mechanism—quantitatively defined in Eq. (6)—which integrates the topology-based distribution index and the net compensation capability into a single composite partitioning index as follows:

$$\sigma = w_1 R_{\text{distance}} + w_2 R_{\text{net}} \tag{6}$$

where w_1 and w_2 are the weighting coefficients for the initial node distribution metrics and the net compensation capability, respectively, is fixed based on iterative parameter tuning.

2.2 Cluster Partitioning Metrics

2.2.1 Power Balance Metrics

The cluster partitioning metrics presented in Sections 2.2.1–2.2.3 are adapted from [7]. Based on these metrics, an original weighted integration strategy is further proposed in Section 2.2.4 to construct a comprehensive clustering coefficient.

The high penetration of Distributed Generation (DG) and EV/EC has intensified bidirectional power flows, rendering traditional clustering methods insufficient to address challenges such as reverse power flow and voltage violations. To maintain dynamic active and reactive power balance within each cluster, it is essential to quantify both active power self-sufficiency and reactive power regulation capability. Reverse power flows significantly increase line losses and elevate the risk of equipment overload, while voltage violations require mitigation through adequate local reactive compensation margins. This metric assesses intra-cluster power consistency by calculating the net active power exchange demand and the proportion of available reactive power compensation. It provides dynamic guidance for the clustering process, promoting optimal spatiotemporal coordination between sources and loads. The formulation is defined as follows:

$$\alpha_P = \frac{1}{K}\sum_{s=1}^{K}\left[1 - \frac{1}{T_{\text{in}}}\sum_{t\in T_{\text{in}}}\frac{P_{\text{net},s}(t)}{\max\left(P_{\text{net},s}(t)\right)}\right] \tag{7}$$

$$\alpha_Q = \frac{1}{K}\sum_{s=1}^{K}\begin{cases}\dfrac{Q_{sup,s}}{Q_{\text{need},s}} & Q_{sup,s} < Q_{\text{need},s} \\ 1 & Q_{sup,s} \geq Q_{\text{need},s}\end{cases} \tag{8}$$

$$\alpha = \frac{\alpha_P + \alpha_Q}{2} \tag{9}$$

where $P_{\text{net},s}(t) = \max(0, P_{load,s}(t) - P_{need,s}(t))$ is the net active power compensation capacity of nodes in cluster s at time t. $Q_{\text{sup},s}$ and $Q_{\text{need},s}$ are the maximum reactive power output and demand of cluster s over the time window T_{in}. α_P and α_Q are the system-wide active and reactive power balance indices, when reactive demand dominates, increasing the weight of α_Q in (9) improves compensation performance.

2.2.2 Node Affiliation Metrics

Cluster size uniformity directly affects the efficiency of hierarchical control. Oversized clusters can trigger the "curse of dimensionality" in centralized optimization, while undersized clusters often lack sufficient resources, leading to frequent inter-cluster support and weakened autonomy. To address this, the proposed node affiliation metric enforces balance by constraining the variance in cluster size. It replaces traditional direct connection counts with the shortest path edge length $topo_{i,j}$ and quantifies each node's relative affiliation strength using a dynamic ratio, thereby mitigating the destabilizing effects of extreme cluster sizes on the "intra-cluster autonomy—inter-cluster coordination" framework. The formulation is defined as follows:

$$\mu\left(i, C\left(i\right)\right) = \frac{1}{\left|C\left(i\right)\right|} \sum_{j \in C(i)} \frac{1}{topo_{i,j}} \tag{10}$$

$$\mu\left(i, C - C\left(i\right)\right) = \frac{1}{\left|C - C\left(i\right)\right|} \sum_{j \in C - C(i)} \frac{1}{topo_{i,j}} \tag{11}$$

$$\beta = \frac{1}{N} \sum_{i=1}^{N} \text{normalize}\left(\frac{\mu\left(i, C\left(i\right)\right)}{\mu\left(i, C - C\left(i\right)\right)}\right) \tag{12}$$

where $C(i)$ is the cluster of node i. $|C(i)|$ is the total number of edges among nodes in $C(i)$. $j \in C(i)$ are nodes connected to i within the same cluster. $\mu(i, C(i))$ is the affiliation degree of node i with its connected nodes in $C(i)$. $C - C(i)$ denotes all clusters excluding $C(i)$. $|C - C(i)|$ is the total number of edges among nodes in the remaining clusters. $J \in C - C(i)$ are nodes connected to i but outside $C(i)$, and $\mu(i, C - C(i))$ is their affiliation degree.

2.2.3 Electrical Modularity Metrics

Evaluating cluster structural performance based solely on the topological relationships among distribution network nodes overlooks the critical electrical interdependence between them. To address this limitation, most existing studies introduce the following formulation to quantify the degree of electrical coupling between nodes:

$$d_{i,j,t} = \log_{10}\left(\frac{S_{QV,t}\left(j, i\right)}{S_{QV,t}\left(i, j\right)}\right) \tag{13}$$

where $S_{QV,t}(i, j)$ denotes the sensitivity matrix at time t, representing the voltage variation at node i caused by a unit change in reactive power at node j. $d_{i,j,t}$ refers to the ratio of voltage variations between node i and node j due to changes in reactive power at node j at time t.

Given that the electrical distance between two nodes is influenced not only by their direct interaction but also by the overall system configuration, the electrical distance between nodes i and j at time t, denoted as $L_{i,j,t}$, is defined as follows:

$$L_{i,j,t} = \sqrt{\sum_{k=1}^{N} \left(d_{i,k,t} - d_{j,k,t}\right)^2} \tag{14}$$

where $L_{i,j,t}$ representing the electrical distance between nodes i and j at time t, implies that a larger value corresponds to a lower edge weight in the modularity function, thus, the relationship between edge weight and electrical distance is defined as follows:

$$e_{i,j,t} = 1 - \frac{L_{i,j,t}}{\max\left(L_{i,j,t}\right)} \tag{15}$$

In this study, a modularity function based on electrical distance is employed to evaluate the structural robustness of the clusters. The modularity concept, originally proposed by Newman, measures the strength of community structures within complex networks. A higher modularity index indicates stronger intra-cluster electrical coupling. The modularity metric is defined as follows:

$$k_{i,t} = \sum_{j=1}^{N} e_{i,j,t} \quad m_t = \frac{1}{2}\sum_{i=1}^{N} k_{i,t} \quad \phi_{i,j,t} = \begin{cases} 1 \text{ node } i, j \text{ belong to the same cluster} \\ 0 \text{ node } i, j \text{ not belong to the same cluster} \end{cases} \tag{16}$$

$$Q_t = \frac{1}{2m}\sum_{i=1}^{N}\sum_{j=1}^{N}\left(e_{i,j,t} - \frac{k_i k_j}{2m}\right)\phi_{i,j,t} \tag{17}$$

$$\gamma = \frac{1}{T_{\text{in}}}\sum_{t\in T_{\text{in}}} \text{normalize}\left(Q_t\right) \tag{18}$$

where $k_{i,t}$ represents the sum of all edge weights connected to node i at time t. m_t is the total sum of edge weights for all nodes in the system at time t. $\phi_{i,j,t}$ indicates whether nodes i and j belong to the same cluster. Q_t denotes the electrical modularity index at time t.

2.2.4 Comprehensive Cluster Partitioning Metrics

It is important to note that the metrics discussed above may exhibit nonlinear trade-offs—for instance, optimizing for high electrical modularity may compromise power balance, while enforcing strict size constraints could restrict the optimization of electrical coupling. To reconcile these competing objectives, a comprehensive index is formulated as a weighted multi-objective function that dynamically balances structural rationality with operational controllability. The expression is defined as follows:

$$\tau = w_1\alpha + w_2\beta + w_3\gamma \tag{19}$$

where w_1, w_2, and w_3 denote the weighting coefficients for the corresponding metrics, all indicators have been normalized.

These multidimensional metrics provide a quantitative basis for selecting initial nodes and support dynamic weight adjustment in the VMCS algorithm's fitness function, as discussed in Section 3.1.

3 Cluster Partitioning Algorithms

To improve adaptability and stability across multi-timescale operations, this paper proposes a hierarchical, progressive dynamic clustering framework [16]. In the spatial dimension, the VMCS algorithm generates a topologically balanced initial scheme, ensuring spatial uniformity and resource balance. Building on this, the CCE-SAO algorithm integrates capacity correction with topology-aware mechanisms to refine node assignments, enhancing structural flexibility and robustness. By embedding time-series features, the algorithm adaptively adjusts cluster boundaries under dynamic conditions.

3.1 Variant Monte Carlo Sampling Algorithm

In dynamic clustering, effective allocation of initial nodes is fundamental to clustering and optimization [17]. This allocation must account for spatial distribution and resource balance. The VMCS algorithm

initializes a population and applies mutation operations inspired by genetic algorithms [18] to iteratively improve the initial solution.

3.1.1 Monte Carlo Sampling Algorithm

In this study, the Monte Carlo algorithm [19] serves as the core method for generating the initial population, aiming to identify the optimal set of initial nodes for each cluster. Initial nodes are generated using a randomized strategy combined with probabilistic distribution. Specifically, the first initial node of each cluster is selected by maximizing its topological distance from the initial node of the preceding cluster, ensuring a spatially uniform distribution of clusters across the network. The algorithmic procedure is outlined as follows:

The candidate population is initialized by randomly generating initial node sets for K clusters in each candidate solution $x_i \in X$.

$$x_i = [I_1, I_2, \ldots, I_K] \tag{20}$$

where $I_k = [n_{k,1}, n_{k,2}, \ldots, n_{k,Nk}]$ denote the initial node set for cluster k. K represents the total number of clusters. N_k denotes the number of initial nodes.

The candidate population is generated as follows:

For generating initial nodes, when $k = 1$, the first initial node is uniformly sampled from the set of unused nodes. For $k > 1$, the sampling probability is dynamically adjusted based on the minimum topological distance to the preceding cluster, with nodes selected according to this adjusted probability distribution. This dynamic sampling probability P_i is calculated to maintain spatial balance for the first initial node in each cluster.

$$P(n_{k,1} = i) = \frac{1}{|Anodes|} \quad k = 1 \tag{21}$$

$$P(n_{k,1} = i) = \frac{\min\limits_{j \in c_{k-1}} topo(j, i)}{\sum\limits_{i' \in Anodes} \min\limits_{j \in c_{k-1}} topo(j, i')} k > 1 \tag{22}$$

$$\sum_{i=1}^{m-1} P_i \le u \le \sum_{i=1}^{m} P_i \quad n_{k,1} = n_m \tag{23}$$

where *Anodes* represent the set of unused nodes. $P_i = P(n_{k,1} = i)$ denote the probability of selecting node i as the first initial node for cluster k. $u = U \sim (0, 1)$. n_m refers to the m-th node satisfying the sampling condition.

For selecting subsequent nodes beyond the first in each cluster, a dedicated strategy is applied.

$$Cnodes = \{i \mid \exists n_{k,l}, topo(n_{k,l}, i) \le 1, \forall l < j)\} \tag{24}$$

$$n_{k,l} = U \sim (Cnodes) \tag{25}$$

Finally, the fitness of the generated initial node configuration is evaluated using the following expression:

$$F_i = f(x_i) \tag{26}$$

where $f(x)$, which corresponds to the comprehensive metrics for initial cluster node allocation defined in Eq. (6).

3.1.2 Constructing the Variant Algorithm

While Monte Carlo-based population generation introduces solution diversity through probabilistic sampling, it can result in solution clustering within local regions. Additionally, solutions derived solely from probability distributions may exhibit low fitness. To overcome these limitations, this study incorporates a mutation-based optimization procedure inspired by genetic algorithms [20] to further refine the population. The mutation process is described as follows:

For each cluster within a candidate solution $x_i \in X$, a mutation operation updates the initial nodes. Boundary nodes are the initial nodes I_k in a cluster that connect topologically to only one other node within the same cluster. The mutation strategy randomly selects a boundary node n_{del} and replaces it with an unused node n_{new} that is topologically adjacent to the current cluster. The chosen n_{new} must satisfy both topological and capacity constraints to avoid disconnection caused by isolated nodes.

$$Enodes = \left\{ i \in c_k \left| \left| j \in c_k \neg \{i\} \ | topo_{i,j} \leq 1 \right\rangle \right| = 1 \right\rangle \right\} \tag{27}$$

$$n_{\text{new}} = \text{rand} \left\{ i \mid \min_{j \in c_k \neg \{n_{del}\}} topo\,(i,j) = 1 \right\rangle \right\} \tag{28}$$

$$c_k = \left(c_k \neg \{n_{\text{del}}\}\right) \cup \{n_{\text{new}}\} \tag{29}$$

Each candidate solution x_i undergoes multiple mutations, with the best solution and its fitness recorded. The solution with the highest fitness F is selected as the initial node configuration for cluster formation.

$$x_i^{\text{best}} = \arg \max_{x_i^{\text{mutated}}} f\left(x_i^{\text{mutated}}\right) \tag{30}$$

$$x^{\text{final}} = \arg \max_{x_i} F_i \tag{31}$$

3.2 Capacity-Corrected K-Means Extension Combined with a Simulated Annealing Optimization Algorithm

3.2.1 Allocation of Initial Cluster Nodes

The initial nodes identified by the VMCS algorithm have globally optimal characteristics. Using them as the starting point for cluster formation narrows the search space and improves partitioning quality and efficiency.

For each cluster $k \in \{1, 2, \ldots, K\}$, the initial nodes $I_{i,k}$ determined by VMCS are assigned to cluster k.

$$C_{I_{i,k}} = k, \forall i \in \{1, 2, \ldots, C_{\text{initial}}\}, \forall k \in \{1, 2, \ldots, K\} \tag{32}$$

$$C_i = \begin{cases} k & \text{node } i \text{ belong to the } k\text{–th cluster} \\ 0 & \text{node } i \text{ remains unassigned} \end{cases} \tag{33}$$

where $I_{i,k}$ denotes the node index of the i-th initial node in the k-th cluster.

3.2.2 Capacity-Corrected K-Means Extension Algorithm

A dynamic cluster expansion method inspired by K-means [21] is enhanced with a capacity correction mechanism to guide node expansion and optimize load distribution. Nodes are pre-allocated based on topological distance, with initial nodes as centroids. Boundary node allocation and capacity correction iteratively refine assignments to keep clusters within size limits. A stochastic selection mechanism offsets topological dominance, promoting balanced and adaptive configurations. The algorithm is outlined as follows:

(1) Topological Distance-Based Node Pre-Allocation:

$$d_{\min\limits_{i\in U}}(i,k) = \min_{j\in S_k} topo(i,j), \forall k \in \{1,2,\ldots,K\} \tag{34}$$

$$CK_i = \left\{ k \,|d_{\min}(i,k) = \min_{j\in\{1,2,\ldots,K\}} d_{\min}(i,j) \right\} \tag{35}$$

$$\begin{cases} C_i = CK_i \,|CK_i| = 1 \\ B = B \cup i \,|CK_i| > 1 \end{cases} \quad i \in U \tag{36}$$

where $U = \{i \in \{1, 2, \ldots, N\}: C_i = 0\}$. S_k denotes the node set of cluster k, defined as $S_k = \{i \,|C_i = k\}$. B denotes the boundary node set, initially empty.

(2) Regular Boundary Node Assignment:
For each boundary node $i \in B$, identify its set of assignable clusters and perform the allocation accordingly.

$$V_i = \{k \in CK_i \,||C_k| < C_{\max}\rangle\} \tag{37}$$

$$C_i = \text{rand}(V_i) \tag{38}$$

where $C_{\max}$ represents the maximum allowable node count for each cluster. If $V_i = \varnothing$, mark node u as an exceptional boundary node and record its associated cluster set CK_u.

(3) Exceptional Boundary Node and Over-Capacity Cluster Handling:
For each exceptional node u, randomly select a cluster $k \in CK_u$ and assign node u to cluster k, even if this exceeds the cluster's capacity limit. Subsequently, remove cluster k from CK_u. If cluster k is successfully processed in later steps, mark node u as resolved. If not, reassign node u to a randomly selected cluster in CK_u. If only one candidate remains in CK_u, force the assignment and mark the node as resolved.

(4) Over-Capacity Cluster Adjustment:
For each cluster k exceeding $C_{\max}$, repeat the following until $|C_k| \lesssim C_{\max}$ or a maximum number of iterations is reached.
Identify boundary nodes E_k of cluster k, randomly select a node $i \in E_k$, and determine the adjacent node set N_i. Then, identify the set W_i of neighboring clusters with available capacity.

$$E_k = \left\{ i \in S_k \,|\left| j \in S_k \neg \{i\} \,|topo_{i,j} \le 1 \right\rangle| = 1 \right\rangle\} \tag{39}$$

$$N_i = \{j \,|topo(i,j) = 1\rangle\} \tag{40}$$

$$W_i = \left\{ C_j \,|j \in N_i, C_j \neq k, \left|S_{C_j}\right| < C_{\max} \right\rangle\} \tag{41}$$

(5) Cluster Update:
If $W_i \neq \varnothing$, assign node i to the cluster $k' \in W_i$ with the largest remaining capacity. If $W_i = \varnothing$, select another node i from the remaining boundary nodes in E_k and repeat the procedure.

$$C_i = k' \,|S_k| = |S_k| - 1 \,|S_{k'}| = |S_{k'}| + 1 \tag{42}$$

(6) Final Verification:

$$\forall i \in \{1, 2, \ldots, N\}, C_i \neq 0 \tag{43}$$

$$\forall k \in \{1, 2, \ldots, N\}, |S_k| \le C_{\max} \tag{44}$$

3.2.3 Topology-Aware Dynamic Optimization of Cluster Nodes

A topology-aware dynamic node optimization mechanism reassigns boundary nodes and their neighbors to improve clustering quality and approach a global optimum. Stochastic elements foster diverse optimization paths. The mechanism targets boundary nodes in interaction zones between adjacent clusters, using topological adjacency to guide reassignment while enforcing capacity constraints. Through localized iterative optimization, clusters are incrementally refined toward balanced configurations and improved partitions. The single-iteration algorithm proceeds as follows:

(1) Boundary Node Selection and Neighbor Identification:

Randomly select a target cluster C_k, identify its boundary node set E_k according to Eq. (39), and randomly select a boundary node e. If $E_k = \varnothing$, set $e = 0$. If $e \neq 0$, compute the set W_e of neighboring nodes adjacent to e but belonging to other clusters using Eq. (41), then randomly select a neighboring node n and let C_n denote its associated cluster. If $W_e = \varnothing$, set $n = 0$.

(2) Stochastic Node Reallocation Strategy:

Randomly choose an operation type with *action* = rand(1, 2). If $e = 0$ or $n = 0$, the node exchange operation is considered invalid. If *action* = 1, migrate the boundary node to the neighboring node's cluster according to Eq. (45); if *action* = 2, reassign the neighboring node to the boundary node's cluster according to Eq. (46).

$$\text{if} \begin{cases} |C_n \cup \{e\}| \leq C_{\max} \\ |C_k \neg \{e\}| \geq C_{\min} \end{cases} \quad C_e = C_n \tag{45}$$

$$\text{if} \begin{cases} |C_k \cup \{n\}| \leq C_{\max} \\ |C_n \neg \{n\}| \geq C_{\min} \end{cases} \quad C_n = C_e \tag{46}$$

3.2.4 Topology-Aware Dynamic Optimization via Simulated Annealing

Building upon the VMCS algorithm, this study introduces a novel cluster partitioning approach, termed CCE-SAO, which integrates a capacity-constrained K-means expansion with simulated annealing-based global optimization. Utilizing the initial node sets derived from VMCS, the CCE-SAO framework executes multi-stage dynamic adjustments and iterative refinements, enabling efficient and adaptive clustering under complex operational constraints.

The process begins with a K-means-inspired expansion phase, in which unassigned nodes are allocated to clusters based on the initial configuration. To address potential capacity violations during this expansion, a dedicated correction mechanism is employed. This mechanism enforces strict adherence to capacity limits through targeted boundary node migration and probabilistic reassignment. Following this expansion, a topology-aware node optimization procedure is embedded within a simulated annealing framework [22]. Simulated annealing is selected due to its suitability for discrete, topology-constrained optimization problems, where probabilistic acceptance of local perturbations enables effective escape from suboptimal clustering configurations. Unlike population-based heuristics, simulated annealing allows fine-grained, topology-aware node exchanges with limited computational overhead, making it well suited for localized cluster refinement under capacity and connectivity constraints. By embedding topology-aware local perturbations into the simulated annealing process, the proposed method achieves global iterative adjustments while preserving network feasibility.

By integrating these adaptive mechanisms—specifically, capacity correction and topology-guided simulated annealing—the proposed method overcomes key limitations of traditional K-means, such as sensitivity

to initial seed selection and lack of constraint enforcement. It effectively resolves node count imbalances and mitigates the risk of local optima during cluster expansion. Furthermore, by enhancing solution space exploration, the approach alleviates the convergence inefficiencies typically associated with conventional simulated annealing in complex, multi-constrained scenarios.

The detailed steps of the simulated annealing procedure, adapted from [22] to incorporate topology-aware perturbations, are presented in Algorithm 1.

Algorithm 1: Simulated annealing-based optimization

Step 1: Initialization

Set initial solution C (from 3.2.2), initial temperature T, and best reward R_{best}.

Set $R = \text{Reward}(C)$, $R_{\text{best}} = R$.

Step 2: Iterative Process

For each iteration, perform the following steps:

1. Generate new solution:
   $C' = \text{Swap}(C)$
   $R' = \text{Reward}(C')$
2. Acceptance criteria:
   if Check(C') is true and $R' > R_{\text{best}}$ or $\exp[R' - R)/T] > \text{rand}()$, then
   Accept new solution: $C = C'$, $R = R'$
3. Update best solution:
   if $R > R_{\text{best}}$, then
   $C_{\text{best}} = C$, $R_{\text{best}} = R$
4. Temperature update:
   $T = T * \varphi$

Step 3: Termination

Repeat Step 2 until stopping criteria are met (a maximum number of iterations is reached).

Return best solution C_{best}.

Where C denote the initial clustering solution obtained from the cluster refinement procedure in Section 3.2.2, C_i, $i \in \{1, 2, \ldots, N\}$, represents the cluster assignment of node i. Swap(C) denotes the topology-aware dynamic cluster optimization function (from Section 3.2.3). Reward(C) refers to the cluster partitioning objective defined in Eq. (19). Check(C) denotes the constraint verification function. R_{best} represent the best reward value. C_{best} represent the best clustering solution. T is the initial temperature of the simulated annealing algorithm. φ is the cooling rate parameter.

4 Case Study

4.1 Case Study Data

This study uses the IEEE 33-bus distribution system to test two scenarios: high Photovoltaic (PV) penetration and large-scale EV/EC deployment, where battery swapping stations have energy storage. A dynamic, time-varying load clustering model is built under multi-timescale conditions, excluding node 1. The baseline configuration is: PV penetration 14%, peak EV/EC load 112 kW, and SVC regulation ±5 Mvar. The proposed "spatiotemporal collaborative optimization–distributed iteration" HI algorithm is applied in a two-layer control framework. Simulations use MATLAB R2023b. The Monte Carlo algorithm generates 500 candidate populations, followed by 50 mutation operations. During clustering, simulated annealing runs up to 100 iterations with an initial temperature of 100°C and a cooling rate of 0.99.

The system has 32 distribution lines and 33 bus nodes. Besides base loads, it includes 7 PV units, 5 EVs, 3 ECs, 5 ESSs, 3 SVCs, and 5 Capacitor banks (CBs). Idle battery modules in EC stations are treated as storage and incorporated into clustering. The system topology is shown in Fig. 1.

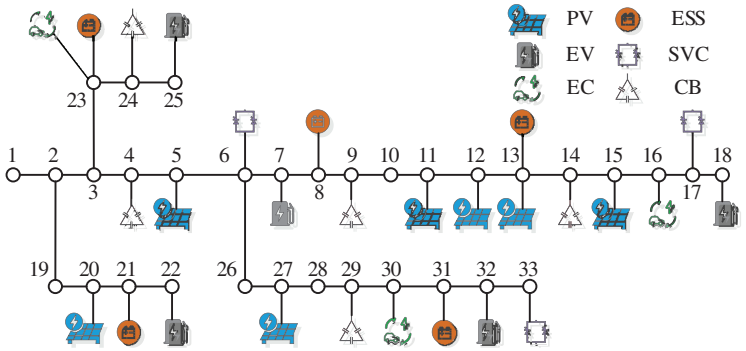

Figure 1: Topology of the 33-bus system.

4.2 Cluster Partitioning Results

Based on the VMCS algorithm, initial nodes are selected considering topological balance and power support capacity. As shown in Fig. 2, initial centers in the IEEE 33-bus system are chosen from nodes with high net compensation and spatially open locations. This strategy balances topological dispersion and power regulation margin, reducing local overload and cluster overlap.

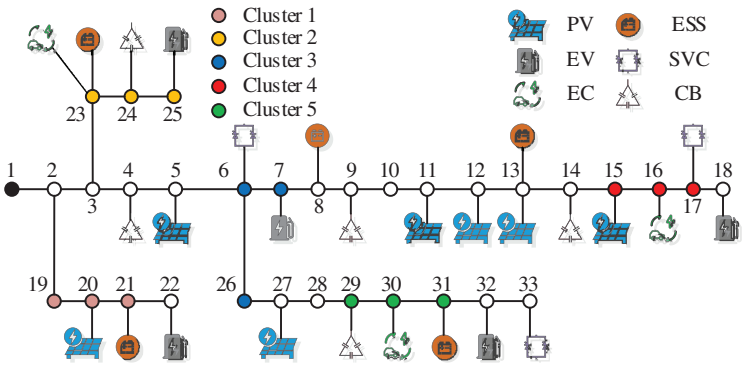

Figure 2: Initial nodes allocation in the 33-bus system.

Building on these centers, CCE-SAO performs dynamic node assignment and boundary adjustments. The final IEEE 33-bus cluster partition is shown in Fig. 3.

4.3 Cluster Partitioning under Complex Scenarios

To test adaptability in complex scenarios, the HI algorithm is applied to the IEEE 123-bus system with large-scale PV and EV/EC integration. Results are shown in Figs. 4 and 5. A modified IEEE 123-bus distribution feeder is adopted, following the model presented in [23], where the original feeder is simplified into a balanced single-phase equivalent. Due to topology simplification and the removal of intermediate nodes, the resulting test system consists of 114 buses. Voltage regulators and capacitor banks are modeled explicitly, while three-phase unbalance and switching devices are neglected to ensure compatibility with the optimization framework.

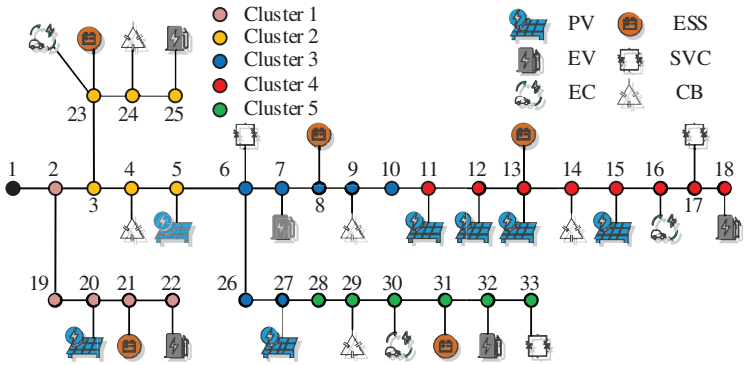

Figure 3: Final cluster partitioning of the 33-bus system.

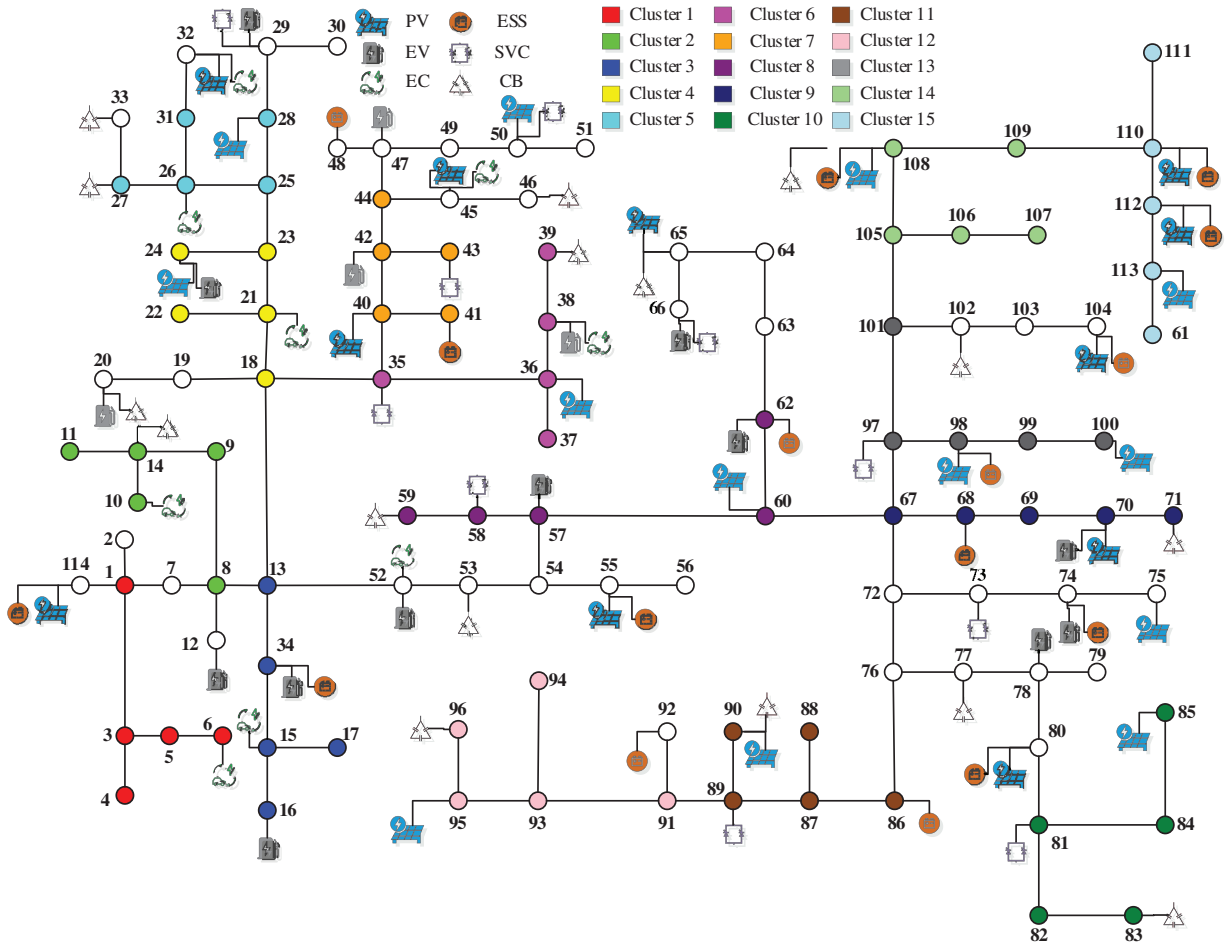

Figure 4: Initial nodes allocation in the 123-bus system.

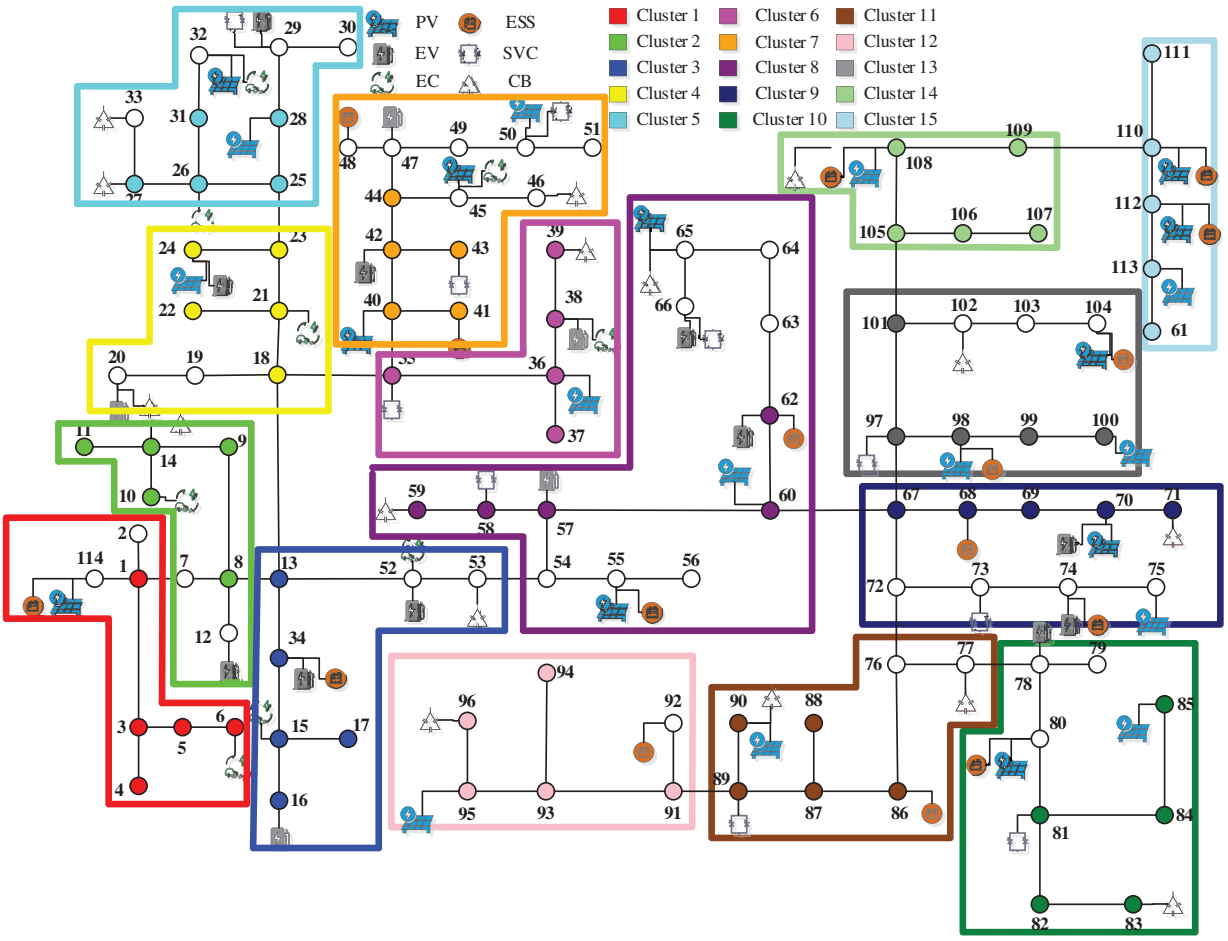

Figure 5: Final cluster partitioning of the 123-bus system.

4.4 Comparative Analysis of Clustering Algorithms

4.4.1 Performance and Feature Comparison

To validate the HI algorithm under large-scale EV/EC integration, clustering performance is evaluated using the proposed metrics. The method is compared with K-means [12], K-medoids [13], and U-SPEC [14]. U-SPEC accounts for topological connectivity and sparsity-based load–compensation balance but its bipartite partitioning can break topology. K-means and K-medoids capture feature similarities but fail to meet both connectivity and dynamic load–compensation demands. A unified evaluation framework is applied across three dimensions: topological connectivity, load–compensation balance, and cluster size uniformity. Results show the limits of single-method approaches to graph–data coupling. The HI algorithm overcomes these by embedding graph-cut optimization into clustering, integrating feature data with topology-aware optimization. Comparative results on the IEEE 33-bus and IEEE 123-bus systems demonstrate its adaptability and expose the strengths and weaknesses of baseline methods in complex scenarios.

Topological Connectivity Constraint: All nodes in a cluster must form a connected subgraph, with at least one intra-cluster path between any two nodes. This prevents isolated subnetworks, ensures power transfer and fault isolation, and avoids control mismatches from segmentation.

Load-Compensation Balancing Consideration: Partitioning accounts for base loads and compensation capacity. An electrical weight matrix matches source, load, and storage, enhancing intra-cluster power balance and voltage regulation while reflecting multi-factor coupling in modern systems.

Cluster Size Constraint: Cluster sizes are kept within thresholds [24], based on automation coverage, distributed generation scheduling, and communication latency.

As shown in Tables 1 and 2, the HI algorithm consistently outperforms K-means, K-medoids, and U-SPEC in clustering metrics for the IEEE 33-bus system. In the IEEE 123-bus system, although the HI algorithm does not achieve the absolute optimal values for all clustering indicators, its performance remains highly competitive with only marginal gaps compared to the best-performing methods, while strictly satisfying all topological connectivity and cluster size constraints. Moreover, the HI framework effectively integrates load–compensation balancing within clusters, ensuring feasibility and coordination under large-scale operating conditions.

Table 1: Performance and feature comparison of clustering algorithms in the 33-bus system.

Clustering Algorithms	HI	K-Means	K-Medoids	U-SPEC
Cluster Partitioning Metrics	0.48	0.46	0.41	0.47
Topological Connectivity Constraint	√	√	×	×
Load-Compensation Balancing Consideration	√	×	√	√
Cluster Size Constraint	√	×	√	×

Table 2: Performance and feature comparison of clustering algorithms in the 123-bus system.

Clustering Algorithms	HI	K-Means	K-Medoids	U-SPEC
Cluster Partitioning Metrics	0.4874	0.4989	0.4882	0.4860
Topological Connectivity Constraint	√	×	×	×
Load-Compensation Balancing Consideration	√	×	√	√
Cluster Size Constraint	√	×	√	×

Note: "√" denotes constraint satisfaction, and "×" denotes constraint violation.

Tables 3 and 4 present node-to-cluster assignments, with initial nodes selected by HI highlighted in red. Detailed node-to-cluster assignments are omitted for brevity; typical partitions are summarized in Tables 3 and 4.

Table 3: Cluster assignment results in the 33-bus system.

Cluster Index	HI	K-Means	K-Medoids	U-SPEC
1	2, 19, 20, 21, 22	2, 3, 19, 20, 21, 22, 23, 24, 25	2, 4, 14, 30	2, 3, 5, 19, 20, 22, 27
5	28, 29, 30, 31, 32, 33	28, 29, 30, 31, 32, 33	7, 8, 25, 26, 31	10, 11, 12, 13, 15, 16, 18, 32

Table 4: Cluster assignment results in the 123-Bus system.

Cluster Index	HI	K-Means	K-Medoids	U-SPEC
1	1, 2, 3, 4, 5, 6, 114	1, 2, 3, 10, 11, 14, 16, 17, 114	2, 5, 7, 10, 12, 17	1, 8, 13, 18, 67
8	54, 55, 56, 57, 58, 59, 60, 62, 63, 64, 65, 66	20, 22, 23, 24, 25, 36, 37, 38, 39, 40, 41, 42	4, 6, 11, 16, 19, 20, 22, 24, 28, 35, 37, 43	29, 35, 43, 50, 58, 66, 73
15	61, 110, 111, 112, 113	61, 110, 111, 112, 113	1, 9, 29, 30, 33, 34, 50, 52, 53, 63, 113	28, 34, 53, 77, 80, 82, 98, 99, 113

Tables 3 and 4 present node-to-cluster assignments, with initial nodes selected by HI highlighted in red. Detailed node-to-cluster assignments are omitted for brevity; typical partitions are summarized in Tables 3 and 4.

4.4.2 Comparison of Voltage Regulation Performance

To evaluate voltage regulation, the HI algorithm is compared with centralized scheduling and three clustering-based methods—K-means, K-medoids, and U-SPEC—on the IEEE 33-bus and 123-bus systems. The voltage regulation performance at the nodes with the largest fluctuations (Node 25 and Node 66) is analyzed. The corresponding scheduling times are also compared to evaluate computational efficiency. Cluster-based scheduling restricts reactive power allocation within each cluster, with no inter-cluster reactive exchange. In this study, cluster capacity is inherently controlled by the cluster planning strategy of the HI framework, which ensures that the number of nodes within each cluster remains within a predefined upper bound. Rather than being enforced through an explicit constraint function, this structural limitation is embedded in the clustering process itself and prevents excessive aggregation of EV/EC-integrated end nodes. Meanwhile, the hard constraints in the reactive power optimization explicitly restrict the balance between the reactive power demand induced by EV/EC charging and the available reactive support within each cluster. Together, these mechanisms limit excessive intra-cluster reactive stress under temporally concentrated EV/EC charging conditions and contribute to improved local voltage regulation. In contrast, conventional clustering approaches such as K-means rely primarily on topological distance during partitioning and do not account for reactive power balance, which may result in clusters that are structurally valid but poorly matched to EV/EC-driven reactive demand.

It should be noted that the proposed framework does not aim to realize fully distributed control. Instead, it adopts a cluster-based centralized optimization strategy, where clustering is used to structurally decompose the original large-scale optimization problem and reduce computational complexity.

As shown in Fig. 6, the HI algorithm outperforms other methods. It is worth noting that the EV/EC charging demand in the studied system exhibits pronounced temporal concentration during both morning and evening peak periods, introducing rapid and localized variations in reactive power demand. Node 25 is a representative end node with EV/EC integration, and although it is not the most fluctuating node at all times, its voltage deviation ranks among the highest across multiple periods. This behavior makes it a suitable reference for evaluating voltage regulation performance under EV/EC-dominated operating conditions. The superior performance of the HI algorithm indicates its enhanced capability to accommodate temporally concentrated EV/EC charging demand and mitigate voltage fluctuations at electrically weak terminal nodes. Regulated per-unit voltage remains between 0.990 and 0.997, with maximum deviation

below 0.5%. Compared to centralized scheduling, it reduces voltage fluctuations by ~30% and achieves higher Electrical Modularity Metrics, indicating stronger intra-cluster coupling, reduced inter-cluster reactive exchange, and enhanced internal voltage stability. By improving dynamic coordination among generation, load, and storage, it enhances local reactive power compensation. In contrast, the original voltage profile (without compensation) shows 0.975–0.995 with significant sags, while K-medoids and U-SPEC violate topological connectivity, yielding profiles similar to the unregulated case, reflecting imbalanced reactive power dispatch.

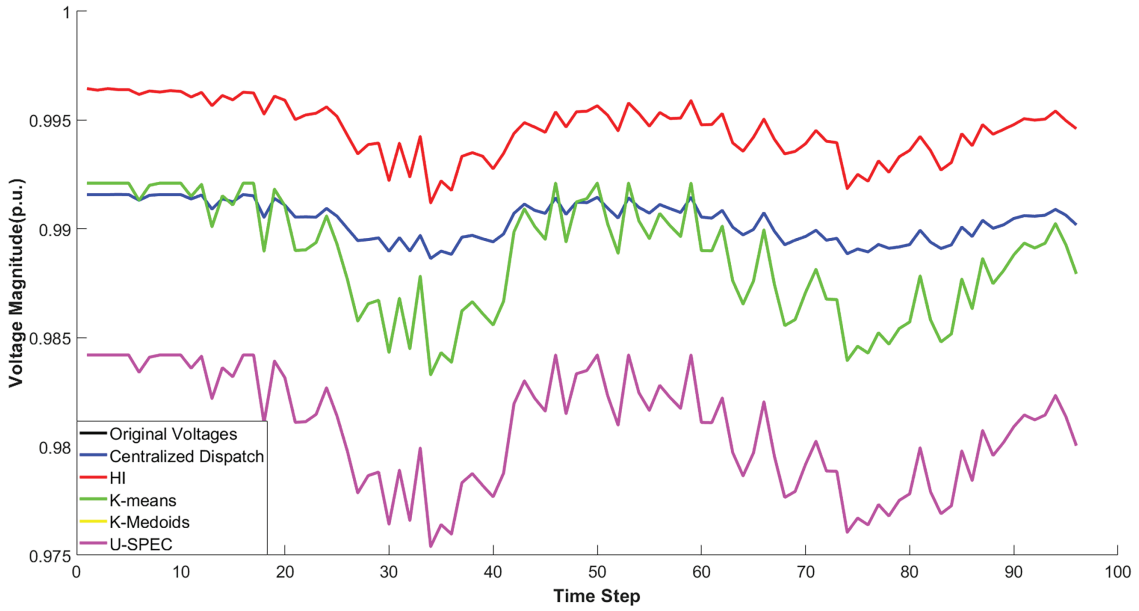

Figure 6: Voltage regulation comparison for the 33-bus system.

In the larger IEEE 123-bus system (Fig. 7), the HI algorithm maintains strong adaptability and outperforms other methods across most evaluation metrics. Per-unit voltage remains highly stable within a narrow range of 0.99979–0.99988. As the system scale increases, the number and spatial dispersion of EV/EC, photovoltaic units, and energy storage systems also grow, resulting in more complex and uncertain spatiotemporal power demand patterns. In the IEEE 123-bus system, Node 66 represents an EV/EC-integrated end node that experiences relatively large voltage fluctuations during multiple operating periods. Under such conditions, centralized scheduling, although capable of achieving the theoretical upper bound of optimization performance, faces challenges in practical deployment due to scalability and responsiveness requirements. By contrast, the hierarchical and progressive structure of the HI framework enables effective coordination within capacity-constrained clusters, allowing it to better absorb localized EV/EC-induced disturbances while maintaining voltage stability. The hierarchical and progressive framework dynamically regulates cluster sizes, mitigating communication delays commonly observed in K-means-based methods and avoiding compensation fragmentation in U-SPEC. In comparison, other clustering-based algorithms fail to preserve strict topological connectivity, which limits their applicability in realistic distribution network environments, whereas centralized scheduling primarily serves as a benchmark for optimal performance.

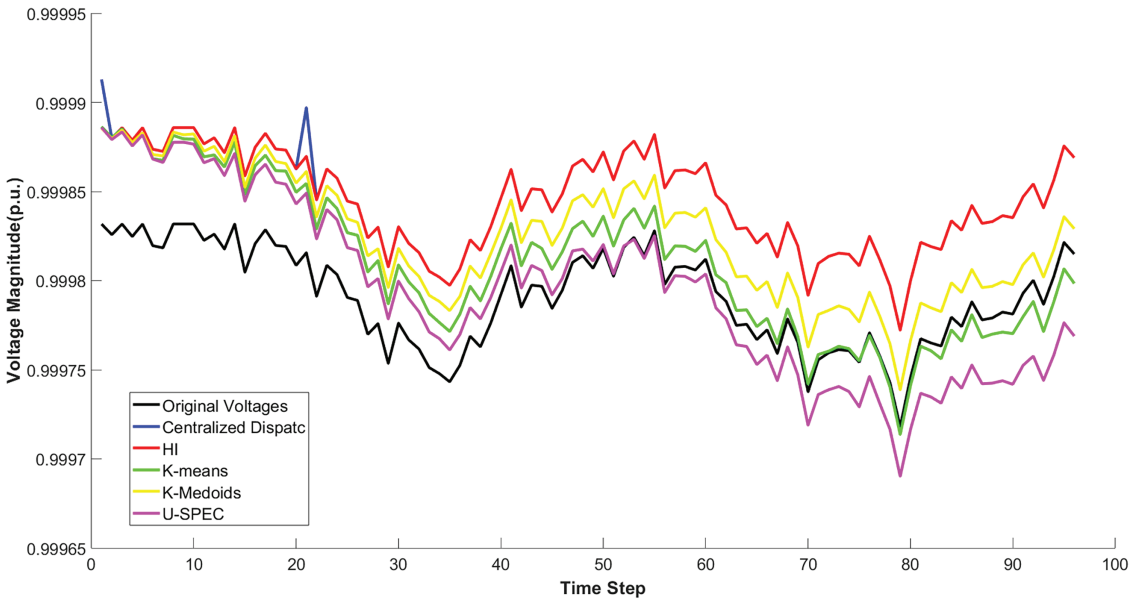

Figure 7: Voltage regulation comparison for the 123-bus system.

Combining Figs. 6 and 7 with Table 5, the HI algorithm demonstrates superior voltage stability, fluctuation suppression, and operational coordination. Cluster-based methods reduce computational overhead compared to centralized scheduling. While HI scheduling time is slightly higher than traditional clustering, this is justified by improved voltage regulation. It should be noted that the IEEE 123-bus system is employed as a large-scale testbed to evaluate the scalability and adaptability of the proposed framework under increased node density and operational complexity. As system scale increases from 33 to 123 nodes, HI scheduling time rises only slightly more than K-means and remains lower than other methods, showing strong scalability and adaptability. Overall, HI ensures effective voltage regulation and exhibits excellent comprehensive performance for large-scale distribution networks.

Table 5: Scheduling time comparison for 33 and 123-bus systems.

Voltage Regulation Method	Centralized Dispatch	HI	K-Means	K-Medoids	U-SPEC
Scheduling Time (s), 33-bus	245.36	80.43	80.02	41.31	32.48
Scheduling Time (s), 123-bus	342.7	270.3	235.8	143.9	234.1

Note: Table values represent the average runtime of voltage scheduling (excluding cluster partitioning) over a 24-h cycle at 15-min intervals, averaged across 10 independent experiments.

5 Conclusion

To address the limitations of static clustering metrics and insufficient global convergence under large-scale EV/EC integration, this paper proposes a hybrid intelligence (HI)-based clustering and optimization framework for distribution networks. The main conclusions are summarized as follows.

(1) A spatiotemporal clustering metric system incorporating spatial topology, net compensation capability, and time-varying load characteristics is proposed. By introducing a dynamic time-coupling factor, the proposed metrics enable clusters to adapt to temporal fluctuations of EV/EC charging demand,

effectively balancing topological proximity and voltage regulation capability. Compared with conventional static or topology-only clustering approaches, this metric system improves responsiveness to distribution network dynamics and mitigates voltage violations under high EV/EC penetration.

(2) A hierarchical and progressive optimization framework combining VMCS and CCE-SAO is developed to enhance clustering robustness and global convergence. VMCS improves the quality of initial node selection by reducing randomness and ensuring spatial balance, while CCE-SAO addresses multi-dimensional capacity constraints through distributed iterations. When integrated with simulated annealing, the framework achieves fast convergence toward global optima and avoids entrapment in local solutions. This two-layer "spatiotemporal coordinated optimization–distributed iteration" architecture fundamentally differs from traditional clustering methods relying on random initialization or single-stage optimization.

(3) Simulation results on the IEEE 33-bus and 123-bus systems demonstrate that the proposed method outperforms centralized scheduling and existing clustering-based approaches in terms of voltage regulation stability. The voltage quality improvement is mainly realized through cluster-constrained optimal scheduling, while clustering provides a topology-consistent and capacity-balanced structure that enhances local reactive power coordination. By enforcing topological connectivity and load–compensation balance within clusters, the method prevents regulation imbalance caused by localized EV/EC aggregation. Moreover, cluster-based scheduling significantly reduces computational burden compared with centralized control, making the framework scalable to large-scale distribution networks. Although the HI-based approach incurs slightly higher scheduling time than some simplified clustering methods, it consistently delivers superior voltage control performance as system size increases.

(4) From a practical perspective, the proposed framework provides meaningful implications for EV/EC infrastructure planning and operation. By identifying regulation-capable clusters and enabling localized reactive power coordination, the method supports high-density EV/EC deployment while alleviating reliance on fully centralized control architectures. This study does not explicitly consider communication latency, which may affect real-time control performance in practical applications. Future work will quantify latency impacts and incorporate them into the clustering metrics, and further extend the framework to multi-feeder distribution networks with over 40% PV and EV/EC penetration to evaluate adaptability under high renewable integration and network reconfiguration scenarios.

Acknowledgement: Not applicable.

Funding Statement: The authors received no specific funding for this study.

Author Contributions: The authors confirm contribution to the paper as follows: conceptualization, Fukang Zhang; methodology, Fukang Zhang; software, Fukang Zhang; validation, Yang Wang, Fukang Zhang and Runtian Tang; formal analysis, Yang Wang, Fukang Zhang and Zhixin Yun; investigation, Fukang Zhang; resources, Yang Wang and Fukang Zhang; data curation, Fukang Zhang; writing—original draft preparation, Fukang Zhang; writing—review and editing, Yang Wang and Fukang Zhang; visualization, Fukang Zhang; supervision, Yang Wang; project administration, Yang Wang. All authors reviewed and approved the final version of the manuscript.

Availability of Data and Materials: The authors confirm that the data supporting the findings of this study are available within the article.

Ethics Approval: Not applicable.

Conflicts of Interest: The authors declare no conflicts of interest.

Appendix A

Appendix A presents the nomenclature used in this paper. Table A1 summarizes all symbols and variables appearing in Sections 2 and 3.

Table A1: Variable table.

Symbol	Description	Unit
$topo_{i,j}$	The topological distance between the initial nodes of cluster i and those of cluster j	/
$P_{\text{sup}}(i, t)$	The active power compensation capacity of node i at time t	W
$P_{\text{load}}(i, t)$	The active power load of node i at time t	W
I_k	The set of initial nodes in cluster k	/
T_{in}	The time interval for cluster partitioning, set to 24 h	/
$P_{\text{net}}(k)$	The total net active and reactive compensation capacities of the initial nodes in cluster k over the period	W
normalize()	The normalization operator	/
K	The total number of clusters	/
$P_{\text{net},s}(t)$	The net active power compensation capacity of nodes in cluster s at time t	W
$Q_{\text{sup},s}$ & $Q_{\text{need},s}$	The maximum reactive power output and demand of cluster s over the time window T_{in}	W
$C(i)$	The cluster of node i	/
$\lvert C(i)\rvert$	The total number of edges among nodes in $C(i)$	/
$j \in C(i)$	Nodes connected to i within the same cluster	/
$\mu(i, C(i))$	The affiliation degree of node i with its connected nodes in $C(i)$	/
$C - C(i)$	All clusters excluding $C(i)$	/
$S_{QV,t}(i, j)$	The sensitivity matrix at time t	/
$k_{i,t}$	The sum of all edge weights connected to node i at time t	/
m_t	The total sum of edge weights for all nodes in the system at time t	/
$\phi_{i,j,t}$	Whether nodes i and j belong to the same cluster	1/0
Q_t	The electrical modularity index at time t	/
N_k	The number of initial nodes	/
$Anodes$	The set of unused nodes	/
$P_i = P(n_{k,1} = i)$	The probability of selecting node i as the first initial node for cluster k	/
n_m	The m-th node satisfying the sampling condition	/
$Cnodes$	Candidate node set for selecting subsequent nodes in a cluster, consisting of unassigned nodes that satisfy predefined topological and constraint conditions	/
$Enodes$	The initial nodes I_k in a cluster that connect topologically to only one other node within the same cluster	/
$I_{i,k}$	The node index of the i-th initial node in the k-th cluste	/

References

1. Hasan KN, Muttaqi KM, Borboa P, Scira J, Zhang Z, Leishman M. Distribution network voltage analysis with data-driven electric vehicle load profiles. Sustain Energy Grids Netw. 2023;36(2):101216. doi:10.1016/j.segan.2023.101216.
2. Then J, Agalgaonkar AP, Muttaqi KM. Coordinated charging of spatially distributed electric vehicles for mitigating voltage rise and voltage unbalance in modern distribution networks. IEEE Trans Ind Appl. 2023;59(4):5149–57. doi:10.1109/TIA.2023.3273186.
3. Dong Q, Zhou G, Huang Q, Dong Z, Jia Y. Resilience enhancement for power distribution networks in coordination with electric vehicle fleets. Appl Energy. 2025;390(5):125756. doi:10.1016/j.apenergy.2025.125756.
4. Zheng S, Liu Y, Fu K, Xiao H, Lin X. Optimal of siting and pricing for multi-type charging facility considering electric vehicle and grid bidirectional power transfer. IEEE Trans Intell Transp Syst. 2025;26(10):17371–85. doi:10.1109/TITS.2024.3460798.
5. Li P, Zhang C, Wu Z, Xu Y, Hu M, Dong Z. Distributed adaptive robust voltage/VAR control with network partition in active distribution networks. IEEE Trans Smart Grid. 2020;11(3):2245–56. doi:10.1109/TSG.2019.2950120.
6. Meng L, Yang X, Zhu J, Wang X, Meng X. Network partition and distributed voltage coordination control strategy of active distribution network system considering photovoltaic uncertainty. Appl Energy. 2024;362(2):122846. doi:10.1016/j.apenergy.2024.122846.
7. Du H, Wei T, Xia D, Zhou S, Han T. Reactive voltage self-regulation and coordination control in distribution networks based on cluster dynamic partition. Autom Electr Power Syst. 2024;48(10):171–81. (In Chinese).
8. Yu H, Wang Y, Wang Q, Cheng Z, Li S, Xiao X, et al. Dynamic network partition and voltage regulation method by PVs considering reactive power compensation benefits. Int J Electr Power Energy Syst. 2025;165(51):110464. doi:10.1016/j.ijepes.2025.110464.
9. Patel S, Murari K, Kamalasadan S. Distributed control of distributed energy resources in active power distribution system for local power balance with optimal spectral clustering. IEEE Trans Ind Appl. 2022;58(4):5395–408. doi:10.1109/TIA.2022.3172391.
10. Liu L, Hu X, Chen C, Wu R, Wu T, Huang H. Research on day-ahead and intraday scheduling strategy of distribution network based on dynamic partitioning. Int J Electr Power Energy Syst. 2024;160(99):110078. doi:10.1016/j.ijepes.2024.110078.
11. Li J, Zhao T, Sun D, Ma J, Yu H, Yan G, et al. Multi-layer optimization method for siting and sizing of distributed energy storage in distribution networks based on cluster partition. J Clean Prod. 2025;501(1):145260. doi:10.1016/j.jclepro.2025.145260.
12. Shahcheraghian A, Ilinca A, Sommerfeldt N. K-means and agglomerative clustering for source-load mapping in distributed district heating planning. Energy Convers Manag X. 2025;25(5):100860. doi:10.1016/j.ecmx.2024.100860.
13. Deng J, Guo J, Wang Y. A Novel K-medoids clustering recommendation algorithm based on probability distribution for collaborative filtering. Knowl Based Syst. 2019;175(12):96–106. doi:10.1016/j.knosys.2019.03.009.
14. Huang D, Wang CD, Wu JS, Lai JH, Kwoh CK. Ultra-scalable spectral clustering and ensemble clustering. IEEE Trans Knowl Data Eng. 2020;32(6):1212–26. doi:10.1109/tkde.2019.2903410.
15. Zhou X, Lu F, Zheng S, Yang Y, Xiang L. Research on the minimum path and Monte Carlo algorithm for reliability of distribution network. IAENG Int J Comput Sci. 2025;52(11):4164–71. doi:10.1201/b12536-12.
16. Wang Y, Pang P, Qi B, Wang X, Zhao Z. A two-stage optimal pre-scheduling strategy for power system inertia assessment and replenishment under extreme weather events. Sustain Comput Inform Syst. 2025;45(2):101079. doi:10.1016/j.suscom.2024.101079.
17. Pan L, Han Z, Shanshan Z, Feng W. An optimal allocation method for power distribution network partitions based on improved spectral clustering algorithm. Eng Appl Artif Intell. 2023;123(4):106497. doi:10.1016/j.engappai.2023.106497.
18. Huang H, Lin T, Zhang X, Liang L, Liu J. Two-layer intelligent planning model of active distribution network based on simulated annealing algorithm and multi-objective function. Comput Electr Eng. 2025;128(5):110733. doi:10.1016/j.compeleceng.2025.110733.

19. Guo Z, Han Q, Wei F, Qi W. Wind power prediction based on hybrid deep learning and Monte Carlo simulation. Eng Appl Artif Intell. 2025;161(1):112082. doi:10.1016/j.engappai.2025.112082.
20. Pesaran HAM, Nazari-Heris M, Mohammadi-Ivatloo B, Seyedi H. A hybrid genetic particle swarm optimization for distributed generation allocation in power distribution networks. Energy. 2020;209(12):118218. doi:10.1016/j.energy.2020.118218.
21. Wang Y, Lai K, Chen F, Li Z, Hu C. Shadow price based co-ordination methods of microgrids and battery swapping stations. Appl Energy. 2019;253:113510. doi:10.1016/j.apenergy.2019.113510.
22. Zhang J, Li Z, Wang B. Within-day rolling optimal scheduling problem for active distribution networks by multi-objective evolutionary algorithm based on decomposition integrating with thought of simulated annealing. Energy. 2021;223(6):120027. doi:10.1016/j.energy.2021.120027.
23. Bobo L, Venzke A, Chatzivasileiadis S. Second-order cone relaxations of the optimal power flow for active distribution grids: comparison of methods. Int J Electr Power Energy Syst. 2021;127(1):106625. doi:10.1016/j.ijepes.2020.106625.
24. Gbadega PA, Sun Y, Balogun OA. Optimized energy management in Grid-Connected microgrids leveraging K-means clustering algorithm and Artificial Neural network models. Energy Convers Manag. 2025;336(13):119868. doi:10.1016/j.enconman.2025.119868.